Nigerian Journal of Science and Engineering Infrastructure (NJSEI)

Volume 1, Issue 1 (2023), 183-194. Musa et al.

Characterization of Bambu Clay as a Precursor for the Synthesis of Zeolite for Catalytic Application

Abdullahi A. Musa [a, d]*, Mohammed U. Garba[a], . Elizabeth J. Eterigho[a], Mohammed Alhassan[a] and Usman Taura[b,c]

[a]Chemical Engineering Department, Federal University of Technology, PMB 65 Minna, Niger State, Nigeria.

[b]Oil and Gas Research Centre, Sultan Qaboos University, Muscat, Sultanate of Oman

[c]Department of Chemical Engineering, University of Maiduguri, P.M.B. 1069, Maiduguri, Nigeria

[d]National Agency for Science and Engineering Infrastructure, P.M.B. 391, Garki-Abuja, Nigeria

Corresponding author: abdulmusavespa@gmail.com

ABSTRACT

The clay in Bambu town, north-central Nigeria, has been used as a ceramic formulation for several generations without understanding its properties. In this paper, the mineralogical study of the Bambu clay sample was investigated in order to deduce its properties and its potential for technological applications. Samples of the clay were first pre-treated and subjected to elemental composition using powder diffraction, morphology, Fourier transform infrared, and area-volume-pore size analyses. The results indicated that Bambu clay can be classified as kaolinite with a Si/Al ratio of approximately 1:85. From the SEM, the particles show the presence of pseudo-hexagonal structures within the clay structure. The average crystallite size was deduced from the XRD analysis to be 43.5nm. The BET analysis reveals that the surface area of the clay was 429.70 m^2g-1, pore volume was 0.042 cm^3g-1 and the pore radius was 2.14 nm. The clay showed that the sample possessed a concentration of Bronsted acidic sites of 31.57 µmol/g and Lewis acidic sites of 34.40 µmol/g. To ascertain the clay's viability for industrial application, the results of the analyses were compared with other clays from the literature. It can be deduced from the analyses that the Bambu clay is kaolinite, mesoporous, has a crystalline structure, a low Si/Al ratio, a higher surface area than zeolite Y, and a high concentration of Lewis acidic sites and a low concentration of Bronsted acidic sites. The clay could be a good precursor material for the synthesis of zeolite Y for catalytic applications.

Keywords: Bambu clay, Kaolinite, Ceramics, Analysis, Zeolite.

INTRODUCTION

Clay minerals are very tiny crystalline substances that evolved primarily from the chemical weathering of certain rock-forming minerals (Holtz *et al*., 2010). The chemical composition and crystalline phases of clay vary according to the geological layer of the soil where they are extracted (Grain 1992). Clay minerals possess plasticity properties when subjected to water and harden when sun-dried. It is composed mainly of grained minerals that make up a colloid fraction with a particle size of about 2 µm (Guggendhein *et al*., 1995). Natural clay is economically attractive as a source for Si and Al and is used as an alternative feedstock for zeolite synthesis (Shanma *et al*., 2010).

DOI.org/10.61352/2023AT11

Clays are hydrous aluminosilicates composed of crystal sheets that have a repeating atomic structure. Tetrahedral silica and octahedral alumina are the two fundamental sheets that exist in clay minerals (Brigetti *et al*., 2006). The tetrahedral sheet consists of silicon-oxygen tetrahedral units (So_4^-) of four oxygen atoms at the corners surrounding a single silicon atom. The octahedral sheet is a combination of octahedral units consisting of six oxygen or hydroxyls enclosing aluminum, magnesium, iron, or other atoms (Sawhnay *et al*., 1989). The sheets are mostly arranged in the 1:1 or 2:1 ratio of silica tetrahedron: alumina octahedron sheets (Brigetti *et al*., 2006). The most common of the 1:1 clay mineral is the kaolinite group which has a chemical formula $Al_2Si_2O_5$ $(OH)_4$. The 2:1 is generally classified as bentonite (Montmorillonite) (Budsacrechai *et al*., 2012).

Kaolinite is a phyllosilicate containing one alumina octahedral layer and a silicon oxide tetrahedral layer. It also comprises non-phyllosilicate minerals such as feldspars, carbonates and quartz together with the oxides of iron and aluminium which are referred to as 'accessory minerals' (Budsacrechai *et al*., 2012) and (Mercier *et al*., 2008). Kaolin clays have repeating layers of one tetrahedral sheet and one octahedral sheet. Kaolinite crystal consists of alternate layers held together by hydrogen bonds between the hydroxyl of the octahedral sheet and oxygen of the tetrahedral sheet. This prevents hydration and allows the layers to stack up to make a rather large crystal up to 70 to 100 layers thick (Holtz *et al*., 2010). The layer thickness of kaolinite is ~0.7nm (Rasheed 2015). Kaolinite is one of the most abundant minerals in soils, mostly easy to mine and it is a common weathering product of many tropical and sub-tropical soils (Bergaya *et al*., 2013). It has versatile uses including; the manufacture of paper, paint, rubber, ceramic, plastic and pharmaceutical products, catalysts for petroleum cracking, auto exhaust emission, control devices, cosmetics base and pigments (Ali 2011). Montmorillonite is the chief mineral in the clay group referred to as bentonite. Bentonite is a subgroup within the smectic clays with the general formula: $M_x(Al_{2-y}Mg_y)Si_4O_{10}(OH)_2.nH_2O$ (Hughes *et al*., 2009) and Belouson *et al*., 2012) while Illites are potassium bentonite with the clay structure general formula $(K,H)Al_2(SiAl)_4O_{10}(OH)_2.XH_2O$ (Olaremu, 2015).

The clay mineral in this study derived its name from Bambu village, which is located in Wamba Local Government Area (LGA) of Nasarawa State, north-central part of Nigeria, and lying between Latitude: 8° 56' 29.51" N and Longitude: 8° 36' 11.34" E. The clay deposit has been mapped over a total area of 1,156 Km^2 (Anudu *et al.,* 2012). Other Prominent mineral deposits in the area include lithium ore and glass sand. The climate of the area is characterized by the rainy season (April to October) and the dry season (November to March) with annual rainfall and temperature varying between 1300mm-1500mm and 28^0C-36^0C respectively (Anudu *et al.,* 2012).
Over the past several decades, the Bambu clay has been used intensively in ceramics formulation and pot-making by the indigenes of Bambu village. Clay mineral has several industrial applications; ceramics, cement, latex, paint, catalysts for petroleum refining, water treatment, cosmetics, etc. The industrial application of clay depends on its mineralogy, chemical composition, mechanical properties (such as plasticity), specific surface area, porosity, surface functionality, acidity sites, and structure (Ihokwene *et al*., 2020).

The objective of this work is to characterize Bambu clay and ascertain its viability for synthesis as a zeolite. This will be achieved through analyses of its structural framework, crystalline phase, quantitative compositions, surface area, and surface functional groups. Though zeolites are crystalline aluminosilicate minerals with distinctive three-dimensional structural shapes that form uniformly sized interconnected pores of molecular dimensions, they are widely used

in industrial applications (Asmaa *et al.,* 2020). Zeolite X and Y are Faujasite classes of zeolites, which are known for remarkable stability and solid structure with large empty spaces (Olaremu, *et al*., 2018). It is widely used in catalytic cracking, hydrocracking, and isomerization processes. Zeolite X has a Si/Al ratio of 1.0–1.5, while Zeolite Y has a Si/Al ratio of 2–5 (Xu, *et al*., 2009).

On the other hand, the importation of zeolite is not encouraging to local content and has an adverse effect on Gross Domestic Product (GDP). Importation of zeolite may not be sustainable because it depends on the foreign market, especially in developing countries. Therefore, there is a need to source locally, especially from raw clay materials, considering the fact that clay is widespread across each geographical location of Nigeria, easily mined at a reasonable cost, almost free to harness, generally non-toxic, and environmentally friendly.

MATERIALS AND METHOD

Materials

A Bambu clay sample was collected from the clay deposits in Wamba LGA at a depth interval of 1.0 -1.5 m with the aid of a shovel and digger. The sample was sorted out by hand to minimize the possibility of contamination with sand. 50 kg of the sample were collected and placed in a polythene bag, which was taken to the Science and Technology Education at the Post-Basic Level (STEP-B) laboratory at the Federal University of Technology (FUT) in Minna for the research study.

Method

10 kg was subjected to preliminary treatment before for characterization to determine its suitability as a precursor for the synthesis of zeolite catalyst. The first step in pretreating Bambu clay was the removal of overburden, vegetation, and other debris associated with the clay deposits. The removal was achieved by rubbing the clay using hands, and thereafter it was dried under the sun at an average sunshine temperature of 36 ^{0}C for one week to reduce the moisture levels and prevent excessive shrinkage or cracking during subsequent processing steps. The clay was further crushed and grinded using a laboratory porcelain pestle and mortar to reduce large particles and agglomerates that needed to be reduced in size to achieve a consistent particle size distribution. After crushing and grinding, the clay was sieved through a 145 µm sieve to remove any larger particles or impurities that weren't broken down effectively and ensure a more uniform particle size distribution. The decomposition of organic matter associated with Bambu clay was conducted by subjecting the clay to heating at a temperature of 60 ^{0}C using a heating mantle so as to drive off volatile organic compounds and moisture in the clay for characterization.

Characterization of Bambu Clay

X-ray Fluorescence (XRF)

The chemical composition of the clay sample was investigated using XRF analysis (Thermo Scientific ARL QUANT'X EDXRF Spectrometer). The analysis was carried out using the standard method and Montana soil SRM 2710 as a Thermo Fisher Scientific standard reference material. Two grammes (2.0 g) of the powdered sample was weighed, poured into a sample holder, covered with cotton wool, and inserted into the XRF Spectrometer for ten minutes after which the result was recorded.

X-Ray Diffraction (XRD)

X-ray Diffraction (XRD) was used to determine the crystal structure and phase identification using the Empyrean Panalytical Multi-Purpose Research X-Ray Diffractometer XRD. A known weight (2.0g) of the sample was powdered, sieved to size (75 µm) and placed in a

sample holder. The voltage and the current of the X-Ray machine were set and the computer software was activated for copper Kα wavelength (Cu K-alpha) of 1.5406 Å. The XRD patterns were recorded on the machine at room temperature within the range of 3 to 90^{o} on the 2θ scale with a scanning speed of 0.05 ^{o}/s.

Brunauer-Emmett-Teller (BET)

The surface area and pore data of the clay sample were investigated using the Brunauer, Emmet and Teller (BET) Nitrogen adsorption technique on NOVA 4200e model equipment. 0.5 g of each sample was measured and inserted in a sample holder. The sample was degassed at 25 ^{0}C for three hours to remove moisture and air. The sample was thereafter analysed for the physisorption of nitrogen gas at a temperature of 273K. The instrument introduced a known quantity of nitrogen gas into the tube while the relative pressure of Nitrogen (P/P_o) was recorded (P = equilibrium gas pressure and P_o = saturation gas pressure). A plot of the specific volume against relative pressure was generated by the machine.

Fourier Transform Infrared Spectroscopy (FTIR)

The FT-IR studies were conducted using the Agilent Cary 630 FTIR spectrometer model. The FT-IR probe was cleaned with ethanol and then baseline run to avoid interference. The spectra were recorded in the region of 4000 - 400 cm^{-1} at a frequency of 50/60 Hz and 110-240VAC.

Scanning Electron Microscopy

The topological and chemical composition of the clay compounds was further confirmed using field emission scanning electron microscopy (FESEM) (JSM-7800F, JEOL, Japan) coupled with an energy dispersive x-ray spectrometer (EDX).

X-ray Photoelectron Spectroscopy (XPS) Analysis

X-ray Photoelectron Spectroscopy (XPS) using multiprobe instrument XPS (Scienta Omicron, Germany) fitted with a hemispherical electron analyzer and operating using Al Kα radiation (h = 1486.6 eV) at 15 kV and 20 mA was utilized under a vacuum condition of 10^{-10} KPa to determine the elemental composition and binding energies of the Bambu clay. The XPS spectra obtained were deconvoluted using CasaXPS program (Casa Software Ltd, UK), in which the background was simulated by the Shirley function while the peaks fitting was achieved using Gaussian Lorentzian function. The binding energy of C1s (284.6 eV) was set as the reference energy.

Pyridine Probe

A pyridine probe was conducted to determine the surface acidity and the clay sites for application as a catalyst. The sample was dissolved in pyridine solution for 24 h then, an Agilent Cary 630 FTIR spectrometer model was used to probe the surface functionally of the clay. The spectra were recorded in the region of 4000 - 400 cm^{-1} at a frequency of 50/60 Hz and 110-240VAC.

RESULTS AND DISCUSSION

X-Ray Fluorescence analysis of raw Bambu clay

The chemical composition of Bambu clay obtained from XRF analysis is presented in Table 1. The XRF analysis of the clay usually indicates the presence of oxides Si and Al (SiO_2 and AlO_3) as they are predominant, having higher percentages than any other oxides. The results of the XRF analysis as presented in Table 1 shows that the Si/Al ratio is 1:80, indicating that the Bambu clay can be classified as kaolinite (Cadene *et al*., 2005). This implies that the structure of the Bambu clay consists of tetrahedral sheets of silica inserting a central octahedral sheet of alumina in the structure (AlO_3).

Table 1.0: XRF analysis of raw Bambu clay

Compound	Raw clay (Bambu)
SiO_2	54.40
Al_2O_3	29.30
Fe_2O_3	4.20
CaO	0.41
V_2O_5	0.029
K_2O	1.76
MnO	0.081
NaO_2	0.80
TiO_2	1.64
P_2O_5	ND
SO_3	ND
CuO	0.028
MgO	0.007
NiO	-
CeO_2	-
ZnO	0.019
Ga_2O_3	0.012
Ta_2O_5	-
Cl	-
LOI(1000^0C)	7.31
Si/Al ratio	**1.85**

LOI = Loss On Ignition
Not Detected = ND

X-ray diffraction of Bambu clay

Figure 1. Presents the X-ray diffractogram of Bambu clay with different peaks, miller indices, and lattice parameters at different diffraction angles and intensities. The first peak at $2\theta = 8.93^0$ indicates the presence of illites although the intensity of the peak was not strong enough to justify the presence of illites in appreciable quantity. The second mineral peak at $2\theta = 12.50^0$ indicates the presence of kaolinite, while the fourth mineral peak at $2\theta = 25.10$ indicates the presence of Albite. The fifth mineral peak at $2\theta = 26.79$, which was the highest intensity on the diffraction pattern of Bambu clay indicates the presence of crystallite silica referred to as Quartz. The high Quartz intensity in clay minerals has previously been reported by other researchers (Jaboyedoff *et al*., 1999). Therefore, based on the analysis, we can conclude that Bambu clay has four minerals namely; Kaolin ($Al_2Si_2O_9$), Quartz (Si_3O_6), Albite ($Na_{1.96}Ca_{0.04}Si_{5.96}Al_{2.04}O_{16}$), and Illite ($K_4Al_{16}Si_8O_{48}$). In addition, the minor peaks of kaolinite are assorted with other minerals found at different Bragg's angles of 20.06, 23.30, 25.10, 26.79, 35.00, 38.50, 55.50 and 63.20.

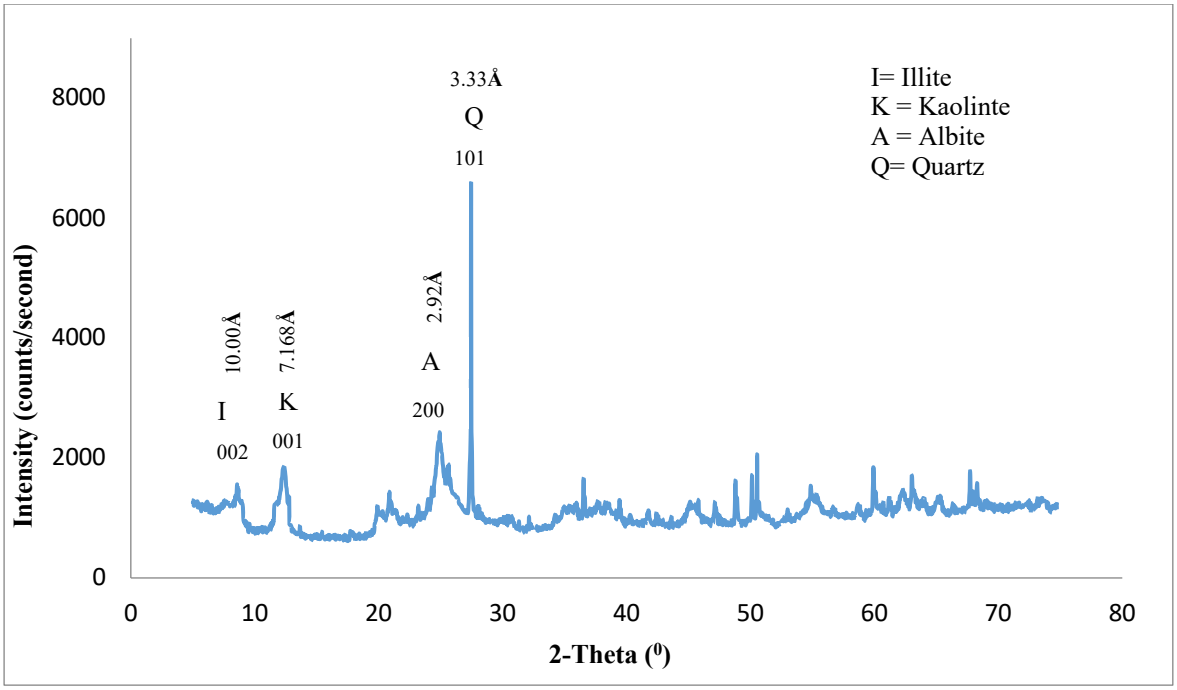

Figure 1.0: XRD pattern of Bambu clay

Crystallite size of the Bambu raw clay generated from the XRD data

The XRD data was further utilized to determine the crystalline size (D) of the raw Bambu clay, using Scherer's equation (equation 1.0). The equation relates the size of crystallites in a solid to the broadening of a peak in a diffraction pattern and is generally used in the determination of a crystal's particle size in a powdered form (Joan *et al*., 2003), (Gorski *et al*., 2010) and (Tzavalas *et al*., 2009).

$$\tau = \frac{K\lambda}{\beta \cos\theta} \quad (1.0)$$

Where τ is the mean size of the ordered (crystalline) domains, K is a dimensionless shape factor (0.9), λ is the X-ray wavelength, β is the line broadening at half the maximum intensity (FWHM), and θ is the Bragg angle.

Table 2.0 presents the crystallite size of the raw Bambu clay in the range of 8.04 - 85.52 nm with an average crystallite size of 43.5 nm and an overall average crystallite size with pore diameter within the range of 2 and 50 nm. Therefore, from this analysis, we can refer to the Bambu clay mineral as mesoporous clay.

Table 2.0: Crystallite size of the raw Bambu clay generated from the XRD data

Diffraction angle 2Θ	**Θ (radians)**	**d-spacing (nm)**	**FWHM (radians)**	**Crystallite size (nm)**
7.845	0.06846054	11.2698	0.007144505	17.71511557
8.834	0.077091193	9.89837	0.006167994	21.07336324
12.3553	0.107820333	7.16641	0.005317146	8.039928525
23.3013	0.203342202	3.81759	0.005702863	23.41088838
24.9281	0.217538711	3.57201	0.008546005	16.62897919
25.7221	0.224467668	3.46352	0.005702863	23.51857313
28.0803	0.245046845	3.17778	0.005866924	16.85756203
30.613	0.267148822	2.92041	0.007144505	18.32360218
35.0066	0.305490215	2.92041	0.005909685	17.06018224

38.5496	0.336408723	2.56329	0.007141015	20.58559254
50.6011	0.4415779	1.8176	0.006604326	23.23999014
58.7474	0.512667778	1.57172	0.006604326	24.11043444
63.1081	0.550722065	1.472	0.008361872	85.51729819
73.7103	0.643243714	1.28427	0.007623598	10.6065098
Average crystallite size				**43.55840261**

Fourier Transform Infrared spectra (FTIR) of Bambu clay

Following the procedure by Uddin *et al*., (2008), FTIR analysis of the clay was conducted at an infrared wavelength of 4000-5000 cm^{-1} to ascertain the various functional groups present in the Bambu clay. Figure 2 shows that the clay has well-resolved (-OH) absorption bands in the IR spectrum at peaks 3695.30, 3626.20, 3402.98, 1620.26, and 799.48 cm^{-1}. These peaks are related to the -OH- stretching vibrating bands in the Bambu clay (Ajayi 2012). The bands indicate the presence of kaolinite as revealed by Frost (1995) and are similar to the results obtained by Patel (2014). The appearance of peaks 1018.45, 799.84, and 678.97cm^{-1} at the low region indicates the presence of Quartz, which agrees with the result obtained by Nwosu et al (2003). Therefore, Bambu clay could be described to contain predominantly kaolinite as confirmed in the previous XRD analysis.

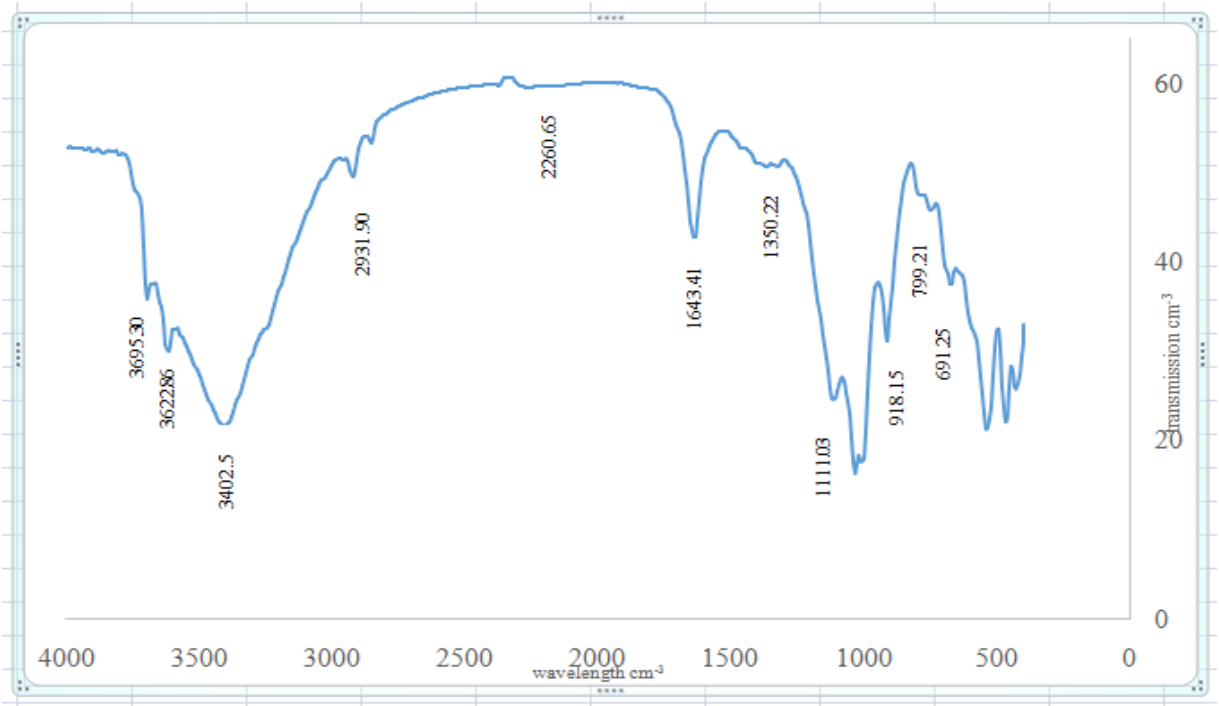

Figure 2: Fourier Transform Infrared spectra (FTIR) of raw Bambu clay

Scanning Electron Microscope (SEM) of Bambu clay

The morphology and the crystallite size of Bambu clay were studied using Scanning Electron Microscopy (SEM) as a complimentary characterisation technique to the XRD analysis. The morphology in Figure 3 shows that Bambu clay contains large stacks of highly packed kaolinite (Earnest *et al*., 2014). The pseudohexagonal shape is also present within the microstructure of the clay which is a characteristic of kaolinite minerals.

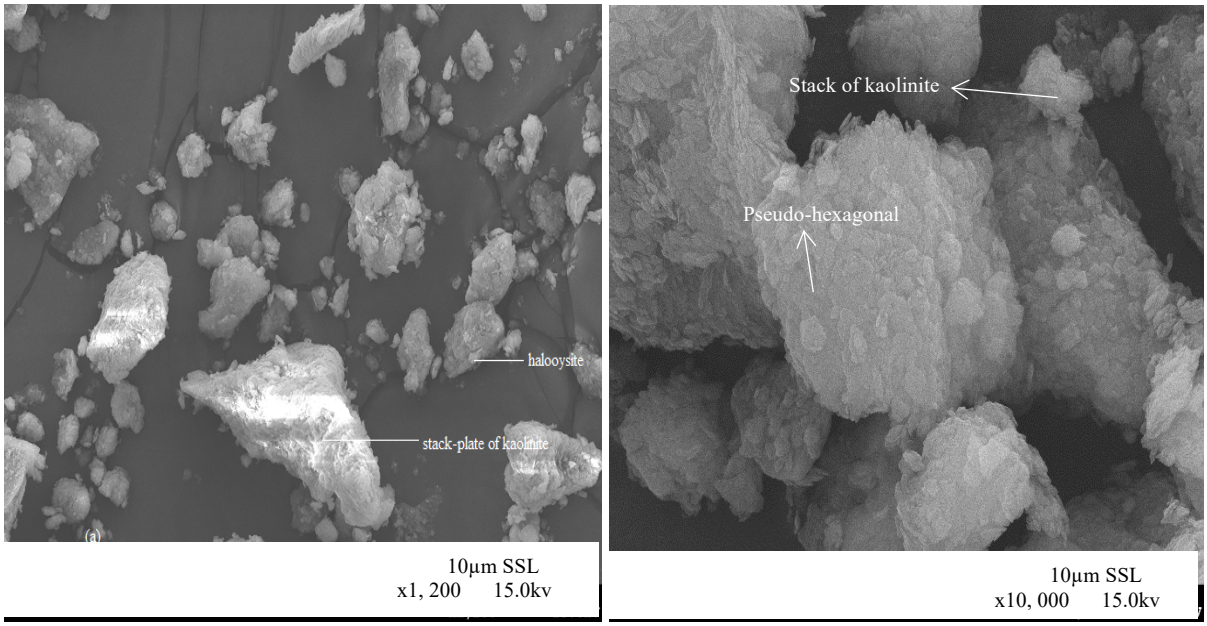

Figure 3: SEM of Bambu Clay

Brunauer-Emmett-Teller (BET) analysis of Bambu clay

The BET analysis was conducted to determine the surface area, pore volume and pore radius of the Bambu clay. Table 3.0 presents the result of the BET analysis of the raw Bambu clay compared to the literature values of the BET of other clays. The result reveals that the clay has a good surface area of up to 429.70 m^2g^{-1}, a pore volume of 0.042 cm^3g^{-1} and a pore radius of 2.14 nm, which was higher, compared to the surface area presented by the research work of Salahudeen (2015). Combining the fact that the average crystallite size of the mesoporous clay is 43nm as revealed by XRD analysis is 43 nm and a relatively good crystallite structure from the BET, we can safely conclude that Bambu clay has the potential for use as a material for absorption, diffusion, and as a catalyst in hydrocarbon cracking (Salahudeen 2015).

Table 3.0: Brunauer-Emmett-Teller (BET) analysis of Bambu clay

Sample	**BET surface Area (m^2/g)**	**Pore Volume (cm^3/g)**	**Pore radius (nm)**
Raw Bambu clay	429.70	0.042	2.14
Literature value	12.95	0.0035	

Pyridine probe acidity test of the Bambu clay

Table 4.0 presents the results of the acidity analysis of Bambu clay indicating the Lewis and Bronsted acidity sites are very low. The result corroborated with the explanation of (Earnest *et al*., 2014) where the ratio of Bronsted/Lewis's acidity site was very low.

Table 4.0: Acidity analysis of the Bambu clay

Samples	Lewis bond (cm^{-1})	Lc Area (µmol)	Bronsted bond (cm^{-1})	Bc Area (µmol)	Lc (µmol/g)	Bc (µmol/g)	Total (µmol/g)	Bc/Lc
Bambu clay	1483.66	5.37	1620.26	3.69	34.40	31.57	65.97	0.92

X-ray Photoelectron Spectroscopy (XPS) of raw Bambu clay

Table 5.0 presents the core-level electron binding energy (eV) of the raw Bambu clay and assigns the respective sub-energy level of the elements. The elements identified by the XPS analysis are O_{1s}, C_{1s}, Si_{2p}, S_{2p}, Al_{2p}, Na_{1s}, Fe_{2p}, K_{2p}, Mn_{2s}, Ca_{2p}, Mg_{1s} and Ti_{2p}, which corroborated with XRF analysis presented in Table 1.0 with carbon being the only exception. However, as described by Meroufel *et al*., (2008) the presence of carbon could be attributed to dried plants or animals, which mix with the clay minerals during clay formation.

Table 5.0: Core-level electron binding energy (eV) of Bambu clay

Element	$1S_1$	$2S_{1/2}$	$2P_{1/2}$	2P	$2P_{3/2}$	$3S_{1/2}$	3P	$3P_{1/2}$	$3P_{3/2}$
C	284								
O	532								
Na	1070	63	31						
Mg	1300	89	52						
Al		118	74	73	73				
Si		149	100	99	99				
K		377	297	294	294	34			
Ca		438	350	347	347	44			18
Ti		564		455	455	59		34	
Fe		846	723	710	710	95		57	
Mn		769	652	641	641	84	49	49	

Discussion

The results of the study provide an understanding of the structural and textural properties of the Bambu clay sample. The Barrett-Joyner-Halenda (BJH) analysis revealed the porous nature of the samples, and the specific surface area of 429.70 m^2/g was calculated to further understand the surface characteristics of the materials. It can be noted that the high specific surface area of the mesoporous silica sample indicates a high number of accessible surface area sites that can be potentially utilized in various applications, such as catalysis, adsorption, and drug delivery. The pore size distribution was also studied and showed that the materials have a range of pore sizes with diameters ranging from 2 to 50 nm, with the majority being in the mesoporous range. This supports the suitability of the material for these applications, as the presence of pores in the mesoporous range is suitable for the encapsulation and controlled release of small molecules (Earnest *et al*., 2014), (Al-Ami *et al*., 2008) and (Nuradeen 2018). The results of the X-ray diffraction analysis showed that the samples have a crystalline structure, with peaks corresponding to the expected crystal phases, a Si/Al ratio of 1.85, which is characteristic of kaolinite, and the morphology showed that the samples contain large pseudohexagonal crystals. The X-ray photoelectron spectroscopy results indicated the presence of various chemical elements on the surface of the materials, with the binding energies of the photoelectrons being determined and showing that the sample possessed concentration of Bronsted acidic sites of 31.57 μmol/g and Lewis acidic sites of 34.40 μmol/g. Overall, this study's characterization shows that the Bambu clay is mesoporous, has a crystalline structure, a low Si/Al ratio, a higher surface area than zeolite Y, as reported by the research work of Nuradden (2018), and a high concentration of Lewis acidic sites and a low concentration of Bronsted acidic sites. This result of Bambu clay corroborates the characteristics results of zeolite Y (low Si/Al of 1.5–3.0, low Bronsted and high Lweis acidic sites, hexagonal, and higher surface area above 400–900 m^2/g) as reported by the research work of Ruren *et al*., (2007) and Asmaa *et al*., (2020). Therefore, Bambu clay could be classified as a potential material for the synthesis of zeolite Y for catalytic applications.

CONCLUSION

This study discussed the analysis of Bambu clay, which has comparable characteristics with other clays. The clay was subjected to preliminary treatment before characterization to determine its suitability as a precursor for the synthesis of zeolite catalyst. The treatment involves the removal of dirty, organic matter and drying it under the sun at an average sunshine temperature of 36 ^{0}C for one week. The clay was further crushed, grinded using a laboratory porcelain pestle and mortar, and sieved through a 145 µm sieve, thereafter subjecting the clay to heating at a temperature of 60 ^{0}C using a heating mantle so as to drive off volatile organic compounds and moisture in the clay for characterization. The XRF analysis indicated that Bambu clay can be classified as kaolinite with a Si/Al ratio of approximately 1:85. From the SEM, the particles show the presence of pseudohexagonal minerals within the clay structure with average crystallite sizes of 43.5 nm, which is a characteristic of kaolin. The BET analysis reveals that the surface area of the clay was 429.70 m^2g^{-1}, pore volume was 0.042 cm^3g^{-1} and the pore radius was 2.14 nm, respectively, which was higher compared to the surface area presented by the research work (Earnest *et al*., 2014), Al-Ami *et al*., 2008) and Nuradeen (2018). The clay showed that the sample possessed a concentration of Bronsted acidic sites of 31.57 µmol/g and Lewis acidic sites of 34.40 µmol/g.

In conclusion, this study demonstrated that the Bambu clay is mesoporous, has a crystalline structure, a low Si/Al ratio, a higher surface area than zeolite Y, and a high concentration of Lewis acidic sites and a low concentration of Bronsted acidic sites. The clay could be a good precursor material for the synthesis of zeolite Y for catalytic applications.

REFERENCE

Ajayi, O., A. (2012). Development of large pore zeolite from kaolinite clays. 226

Asmaa K. B., Helmy E. H., Ahmed A. M., Ahmed M. A., Manar H. M. (2020). Synthesis and characterization of zeolite-Y from natural clay of Wadi Hagul. *Egyptian Journal of Chemistry*. 290.

Al-Ani, T., Sarapaa, O. (2008). Clay and clay mineralogy: physical-chemical properties and industrial uses. *Geological Survey of Finland*. 94.

Ali, O. (2011). Polymer/clay nanocomposites, advances in diverse industrial applications of nano-composites.;

Anudu, G., K., Onuba, L., N., Onwuemesi, A., G., Ikpokonte, A., E. (2012). Analysis of aeromagnetic data over Wamba and its adjoining areas in north-central Nigeria. Earth Sciences Research Journal (ESRJ). 1(1-7).

Belousov, P., E., Pokidko B., V., Zakusin, S., V., Krupskaya, V., V. (2020). Quantitative methods for quantification of montmorillonite content in bentonite clays. *Georesursy*. 22(3):38-47.

Bergaya, F., Lagaly, G. (2013). 2nd ed. Handbook of Clay Science (2). Elsevier Ltd.; 6–29

Brigatti, M., F., Galan, E., Theng, B., K., G. (2006). Structures and mineralogy of clay minerals. *Handbook of Clay Science: Developments in Clay Science.*1-2.

Budsaereechai, S., Kamwialisak, K., Ngernyen Y. (2012). Adsorption of lead, cadmium and copper on natural and acid activated bentonite cla. KKU Res. J. 17(5).

Cadene, A., Durand-Vidal, S., Turq, P., Brendle, J. (2005). Study of individual Na-montmorillonite particle size, morphology and apparent charge. *Journal of Colloid and Interface Science.* 285, 719-730.

Ernest, K., Ngomo1, H., M., Abi, C., F., J., S., N, Sary et al. synthesis and characterization of zeolite y from Akilbenza clay: effect of crystallization time.

Frost, R., L. (1995). Fourier Transform Infrared Spectroscopy of kaolinite, dickite and halloysite. Clays and Clay Minerals. 43(2), 191-195.

Grim, RE. (1962). Applied clay mineralogy.

Guggenheim, S. (1995). Definition of clay and clay mineral: joint report of the AIPEA nomenclature and CMS nomenclature committees. Clay Miner. 43, 255–256.
Gorski C., A., Scherer, M., M. (2010). Determination of nanoparticulate magnetite stoichiometry by Mossbauer spectroscopy, acidic dissolution, and powder X-ray diffraction: A critical review. American Mineralogist. Jul 1. 95(7):1017-26.
Holtz, R., D, Kovacs, WD. (2010). An introduction to geotechnical engineering. New York. Prentice-Hall Civil Engineering and Engineering Mechanics Series; 165-23.
Hughes, J., C., Gilkes, R., J., Hart, R., D. (2009). Intercalation of reference and soil kaolins in relation to physico-chemical and structural properties. Appl. Clay Sci. 45, 24–35.
Ihekweme G., O., Shondo N., J., Orisekeh, K., I., Kalu-Uka, G., M., Nwuzor I., C., Onwualu, A., P. (2020). Characterization of certain Nigerian clay minerals for water purification and other industrial applications. Science Direct. (2)
Jaboyedoff, M., Kübler, B., Thelin, P., H. (1999). An empirical Scherrer equation for weakly swelling mixed-layer minerals, especially illite-smectite. Clay Minerals. Dec. 34(4):601-17.
Joan Z., Hejing, W. (2003). The physical meanings of 5 basic parameters for an X-ray diffraction peak and their application. Chinese journal of geochemistry. Jan;22 (1): 38-44.
Mercier, P., H., Le-Page Y., Tu Y, Kotlyar, L. (2008). Powder X-ray diffraction determination of phyllosilicate mass and area versus particle thickness distributions for clays from the Athabasca oil sands. *Journal of Petroleum science and technology*. 26(3):307-21.
Mignoni, M., L., Petkowicz, D., I,. Machado, N., F., Pergher, S., B., C. (2008). Synthesis of mordenite using kaolin as Si and Al source. Applied Clay Science. (41), 99–104.
Nuradeen S. (2018). Metakaolinization effect on the thermal and physiochemical properties of kankara kaolin. *KMUTNB Int J Appl Sci Technol, vol. 11, no. 2*. 27-135.
Nwosu, D., C., Ejikeme, P., C., N,, Ejikeme, E., M. (2013). Physic-chemical characterization of "NGWO" white clay for industrial use. *International Journal of Multidisciplinary Sciences and Engineering*. 4(3) 11-14.
Olaremu, A.G., Odebunmi, E.O., Nwosu, F.O., Adeola, A.O. and Abayomi, T.G. (2018). Synthesis of zeolite from kaolin clay from Erusu Akoko southwestern. *Journal of Chemical Society of Nigeria*, **43**(3), 381-786.
Olaremu, A., G. (2015). Physico-Chemical Characterization of Akoko Mined Kaolin Clay. *Journal of Minerals and Materials Characterization and Engineering* (3). 353-361.
Patel, H., A. (2014). Nanoclays: synthesis, characterisation and applications. *New Delhi: Astral International Pvt. Ltd*.
Rasheed, B, **(**2015). Development and characterization of *zeolite Y* from a Nigerian local raw material. 26-27
Ruren, X., Gao, Z., Chen, J., Wenfu, Y. (2007). Zeolites to Porous MOF Materials. Journal of material science. 2: 168-414.
Sawhney, B., L. (1989). Interstratification in layer silicates. *Minerals in soil environments.* 789-828.
Salahudeen, N. (2015). Development of zeolite Y and ZSM5 composite catalyst from Kankara kaolin. Department of Chemical Engineering. PhD Zaria: Ahmadu Bello University, Zaria, pp.1-311.
Sharma, S., K., Sambi, S., S. (2010). Conversion of low-grade clays to zeolite NaA. IUP Journal Chemistry. 3, 32–41.
Tzavalas, S., Gregoriou, V., G. (2009). Infrared spectroscopy as a tool to monitor the extent of intercalation and exfoliation in polymer clay nanocomposites. Vibrational Spectroscopy. Sep 18;51 (1):39-43.
Uddin, F., (2008). Nanoclays and montmorillonite minerals. *Metallurgical and Materials Transaction A*. 39. 2804-2814.

Xu, R., Pang, W., Yu, J., Huo, Q. and Chen, J. (2009). Chemistry of zeolites and related porous materials: synthesis and structure. John Wiley & Sons. 34. 231-311